Cell Death and Differentiation (2012) 19, 1896–1907

www.nature.com/cdd

A novel cellular stress response characterised by a rapid reorganisation of membranes of the endoplasmic reticulum

S Varadarajan[1], ETW Bampton[1], JL Smalley[1], K Tanaka[2], RE Caves[3], M Butterworth[1], J Wei[4], M Pellecchia[4], J Mitcheson[3], TW Gant[1], D Dinsdale[1] and GM Cohen*[,1,2]

Canonical endoplasmic reticulum (ER) stress, which occurs in many physiological and disease processes, results in activation of the unfolded protein response (UPR). We now describe a new, evolutionarily conserved cellular stress response characterised by a striking, but reversible, reorganisation of ER membranes that occurs independently of the UPR, resulting in impaired ER transport and function. This reorganisation is characterised by a dramatic redistribution and clustering of ER membrane proteins. ER membrane aggregation is regulated, in part, by anti-apoptotic BCL-2 family members, particularly MCL-1. Using connectivity mapping, we report the widespread occurrence of this stress response by identifying several structurally diverse chemicals from different pharmacological classes, including antihistamines, antimalarials and antipsychotics, which induce ER membrane reorganisation. Furthermore, we demonstrate the potential of ER membrane aggregation to result in pathological consequences, such as the long-QT syndrome, a cardiac arrhythmic abnormality, arising because of a novel trafficking defect of the human ether-a-go-go-related channel protein from the ER to the plasma membrane. Thus, ER membrane reorganisation is a feature of a new cellular stress pathway, clearly distinct from the UPR, with important consequences affecting the normal functioning of the ER.
Cell Death and Differentiation (2012) **19,** 1896–1907; doi:10.1038/cdd.2012.108; published online 7 September 2012

The endoplasmic reticulum (ER) comprises an extensive network of membrane-bound domains that stretches from the inner nuclear envelope throughout the cytosol into the cell periphery, to form ribosome-studded peripheral sheets (rough ER) and interconnected tubules of smooth ER.[1,2] The ER is responsible for important cellular functions including synthesis, folding, modification and secretion of proteins, lipid synthesis, calcium homeostasis and detoxification of xenobiotics.[3,4] The normal functioning of the ER is disrupted in different stress conditions and involves the accumulation of unfolded and misfolded proteins in the ER lumen, which results in the activation of a coordinated intracellular signalling cascade called the unfolded protein response (UPR) to restore cellular homeostasis and integrity.[5,6] The UPR primarily acts as a pro-survival signalling pathway, by temporarily arresting protein synthesis, while simultaneously generating chaperones to aid in proper folding of accumulated luminal proteins. When the stress is overwhelming, the UPR induces C/EBP homologous protein (CHOP), which in turn modulates the levels of pro- or anti-apoptotic BCL-2 family members to eventually eliminate stressed cells.[7,8]

While primarily acting at the mitochondria to regulate apoptosis by controlling the release of cytochrome *c* and other factors, BCL-2 family proteins also localise to the ER where their proposed functions include regulation of calcium release, apoptosis, autophagy and the UPR.[9,10] The differential effect of the UPR on cell survival or death has been attributed to the levels of pro- or anti-apoptotic BCL-2 family members at the ER.[9,10] Anti-apoptotic BCL-2 family members possess a hydrophobic groove that binds and inhibits their pro-apoptotic counterparts, which forms the basis of resistance to chemotherapy.[11] To overcome this resistance and facilitate cell death, small-molecule inhibitors of the BCL-2 family, aimed at dislodging the pro-apoptotic members from the hydrophobic groove, have been developed.[12,13] Some of those molecules, ABT-737 and ABT-263, bind selectively to anti-apoptotic members, BCL-2, BCL-X_L and BCL-W but not to MCL-1 or BCL2A1, whereas other inhibitors, such as apogossypol, TW37 and obatoclax, are considered pan-BCL-2 antagonists.[12,13] Despite the implications of BCL-2 family members in canonical ER stress,[9] only a few reports have attempted to establish a connection between these inhibitors and canonical ER stress.[14] Moreover, as several of these inhibitors are in early clinical trials, it is imperative to gain greater insight into their physiological effects.

In this study, we identify a new form of cellular stress characterised by profound and reversible reorganisation of ER membranes that disrupts normal ER function and occurs

[1]MRC Toxicology Unit, University of Leicester, Leicester, UK; [2]Department of Biochemistry, University of Leicester, Leicester, UK; [3]Department of Cell Physiology and Pharmacology, University of Leicester, Leicester, UK and [4]Sanford-Burnham Medical Research Institute, La Jolla, CA 92037, USA
*Corresponding author: GM Cohen, MRC Toxicology Unit, University of Leicester, Hodgkin Building, PO Box 138, Lancaster Road, Leicester, Leicestershire LE1 9HN, UK. Tel: +44 116 2525609; Fax: +44 116 2525616; E-mail: gmc2@le.ac.uk
Keywords: cell stress; endoplasmic reticulum; MCL-1; membrane reorganisation
Abbreviations: CHOP, C/EBP homologous protein; CLL, chronic lymphocytic leukaemia; ER, endoplasmic reticulum; hERG, human ether-a-go-go-related gene; IRE1α, inositol-requiring protein-1α; LQTS, long-QT syndrome; MCL-1, myeloid cell leukaemia 1; NDGA, nordihydroguaiaretic acid; PERK, protein kinase RNA-like ER kinase; THG, thapsigargin; UPR, unfolded protein response; VSVG, vesicular stomatitis viral glycoprotein; XBP1, X-box-binding protein 1
Received 17.5.12; revised 27.7.12; accepted 27.7.12; Edited by G Melino; published online 07.9.12

independently of the UPR. We further identify MCL-1, together with other BCL-2 family members, to have a key role in the regulation of this novel stress pathway. Using connectivity mapping, we demonstrate the widespread nature of this stress pathway by identifying a range of structurally diverse chemicals capable of inducing ER membrane aggregation. Finally, we establish functional roles for these ER membrane aggregates in the induction of long-QT syndrome (LQTS), a cardiac abnormality that can lead to arrhythmias and death.

Results

Apogossypol induces ER membrane aggregation in an evolutionarily conserved manner. In our previous studies, distinct ultrastructural changes, including mitochondrial swelling and chromatin condensation, were observed when primary chronic lymphocytic leukaemia (CLL) cells were exposed to putative BCL-2 inhibitors.[15] One such inhibitor, apogossypol, induced a profound aggregation of membranous structures resembling a malformed ER network, distinct from the anastomosing ER induced by phenobarbitone[16] and never observed in untreated CLL cells (Figure 1a). Apogossypol induced similar ultrastructural changes in multiple tumour cell lines, including Jurkat T-lymphocytes, HeLa cells, mouse embryonic fibroblasts (MEFs), Chinese hamster ovary cells and even in the fission yeast, *Schizosaccharomyces pombe*, thus establishing the evolutionarily conserved nature of this phenomenon (Figure 1a and Supplementary Figure S1a). ER membrane aggregates were generally apparent within a few hours of treatment, and in some cases, the ER changes were accompanied by dilation of the nuclear envelope and continuity of the outer nuclear membrane with the aggregates was evident (lower panels in Figure 1a).

A dramatic clustering of ER membrane proteins (BAP31/calnexin/reticulon 4), but not proteins associated with early endosomes, lysosomes or mitochondria, was observed in cells exposed to apogossypol (Figure 1b and Supplementary Figure S1b). In these clusters, BAP31 colocalised with other ER-Golgi trafficking proteins, like SEC22 (Supplementary Figure S1b), which were identified as ER membrane aggregates using electron microscopy (Figure 1c), thus validating the use of fluorescence microscopy to monitor this membrane aggregation. BAP31-positive clusters were visible within 1 h of apogossypol exposure and gradually coalesced to form bulkier clusters, in more than 95% of cells, indicating significant aggregation of the extensive ER network (Figure 1d). Despite severe compaction, ER membrane aggregates were highly dynamic and remained connected to the rest of the ER, which was clearly distinct from ER fragmentation, observed in cells exposed to ionomycin[17] (Supplementary Figure S1c). Furthermore, rapid and complete dispersal of the membrane aggregates was observed when apogossypol was washed out (Figure 1e), indicating a reversible reorganisation of the clustered ER membranes.

ER membrane reorganisation causes a functional perturbation of the ER. We speculated that the dramatic reorganisation of ER membranes would result in a trafficking defect and disrupt ER function. Indeed, apogossypol-induced ER membrane reorganisation resulted in a substantial dispersion of the Golgi complex (GM130), indicating a trafficking defect between ER and the Golgi (Figure 2a). Moreover, silencing of genes required for anterograde (αSNAP) or retrograde (syntaxin 18, STX18) trafficking resulted in similar ER changes (Figures 2b and c), supporting the hypothesis that ER membrane reorganisation is associated with disrupted ER-Golgi transport and may be part of a normal homeostatic response. Brefeldin A, which promotes disassembly and rapid trafficking of Golgi proteins back to the ER,[18] completely reversed BAP31 clustering in STX18 downregulated cells, in agreement with previous findings,[19] but did not reverse membrane reorganisation in αSNAP downregulated or apogossypol-treated cells (Figure 2b). These results implied that apogossypol-induced ER membrane reorganisation was associated with defects in anterograde and not retrograde trafficking. To check these findings, we utilised the fluorescently tagged, temperature-sensitive mutant of vesicular stomatitis viral glycoprotein (VSVG). At the non-permissive temperature, VSVG resides exclusively in the ER but is trafficked from the ER to the cell surface *via* the Golgi following a temperature reduction to 32 °C.[20] A complete translocation of VSVG from ER to the Golgi and plasma membrane was observed in control cells, which was abolished in cells exposed to apogossypol (Figure 2d and e). In addition to a trafficking defect, ER membrane reorganisation also resulted in a striking diminution in global protein synthesis, demonstrating a functional perturbation of the ER (Figure 2f).

ER membrane reorganisation occurs independent of the UPR. Canonical ER stress and the UPR are characterised by the activation of specific receptors on ER membranes, including inositol-requiring protein-1 α (IRE1α), protein kinase RNA-like ER kinase (PERK) and activating transcription factor-6 (ATF6).[5,6] While PERK-mediated phosphorylation of eIF2α temporarily arrests ongoing protein synthesis, both ATF6 and IRE1α-mediated truncation of X-box-binding protein 1 (XBP1) generate chaperones like BiP/HSPA5, to aid in protein folding.[1–3] As apogossypol induced extensive ER membrane reorganisation with associated functional defects, we expected this to trigger canonical ER stress. Indeed, exposure to apogossypol resulted in activation of some arms of the UPR, including phosphorylation of eIF2α and CHOP accumulation, with little effect on XBP1 splicing and BiP levels (Figure 3a). However, with the possible exception of eIF2α phosphorylation, the UPR-related changes were detected at much later times (>8 h) than the extensive formation of ER membrane aggregates (<1 h) (compare Figures 1d and 3a). Similarly, comparison of mRNA changes revealed that genes associated with the UPR dominated the top 30 differentially expressed genes following conventional UPR inducers, tunicamycin and brefeldin A, but not in cells exposed to apogossypol for 1 h, despite extensive ER membrane reorganisation (Figures 1d and 3b). Even prolonged exposure to apogossypol (6 h) induced only a few ER stress genes and to a much lower extent than tunicamycin or brefeldin A (Figure 3b). Furthermore, ER membrane reorganisation was evident in the

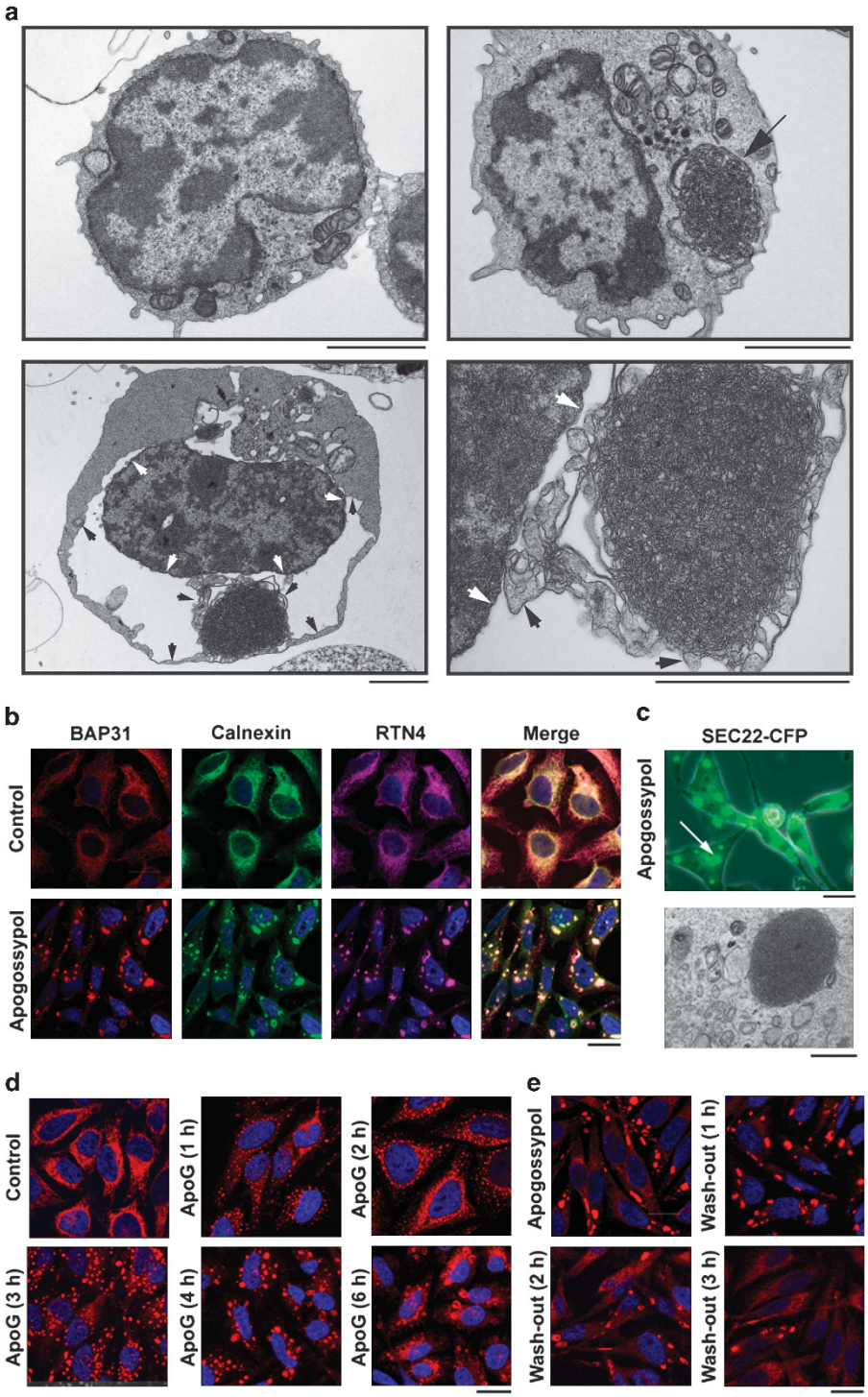

Figure 1 Apogossypol induces a reversible aggregation of ER membranes. (**a**) CLL cells, exposed for 16 h to apogossypol (10 μM), formed membrane aggregates (arrow, top right panel) in contrast to untreated CLL cells (top left panel). Severe swelling of the nuclear envelope was evident in Jurkat cells, exposed for 16 h to apogossypol (10 μM) (lower left panel) and the continuity of this envelope with an ER membrane aggregate is shown at higher magnification (lower right panel) (scale bars, 2 μm). The inner and outer nuclear membranes are indicated by white and black arrowheads, respectively. (**b**) HeLa cells exposed for 4 h to apogossypol (10 μM) and subsequently immunostained for ER membrane proteins (BAP31, calnexin and RTN4) exhibited dramatic clustering of the ER membrane proteins (scale bar, 20 μm). (**c**) Fluorescence microscopy can be used to detect ER membrane aggregates. HeLa cells transfected with CFP-tagged SEC22 and subsequently exposed for 4 h to apogossypol (10 μM) exhibited numerous fluorescent foci. A CFP-labelled cluster (white arrow upper panel, scale bar, 20 μm) was subsequently examined by electron microscopy, establishing that these foci were in fact ER membrane aggregates (lower panel, scale bar 2 μm). (**d**) BAP31-containing ER membrane aggregates undergo time-dependent formation and coalescence in HeLa cells exposed to apogossypol (ApoG, 10 μM) (scale bar, 20 μm). The ER membrane aggregates were visible within 1 h. (**e**) The BAP31-containing ER membrane aggregates, formed in HeLa cells following exposure for 4 h to apogossypol (10 μM), dispersed rapidly on wash out (scale bar 20 μm)

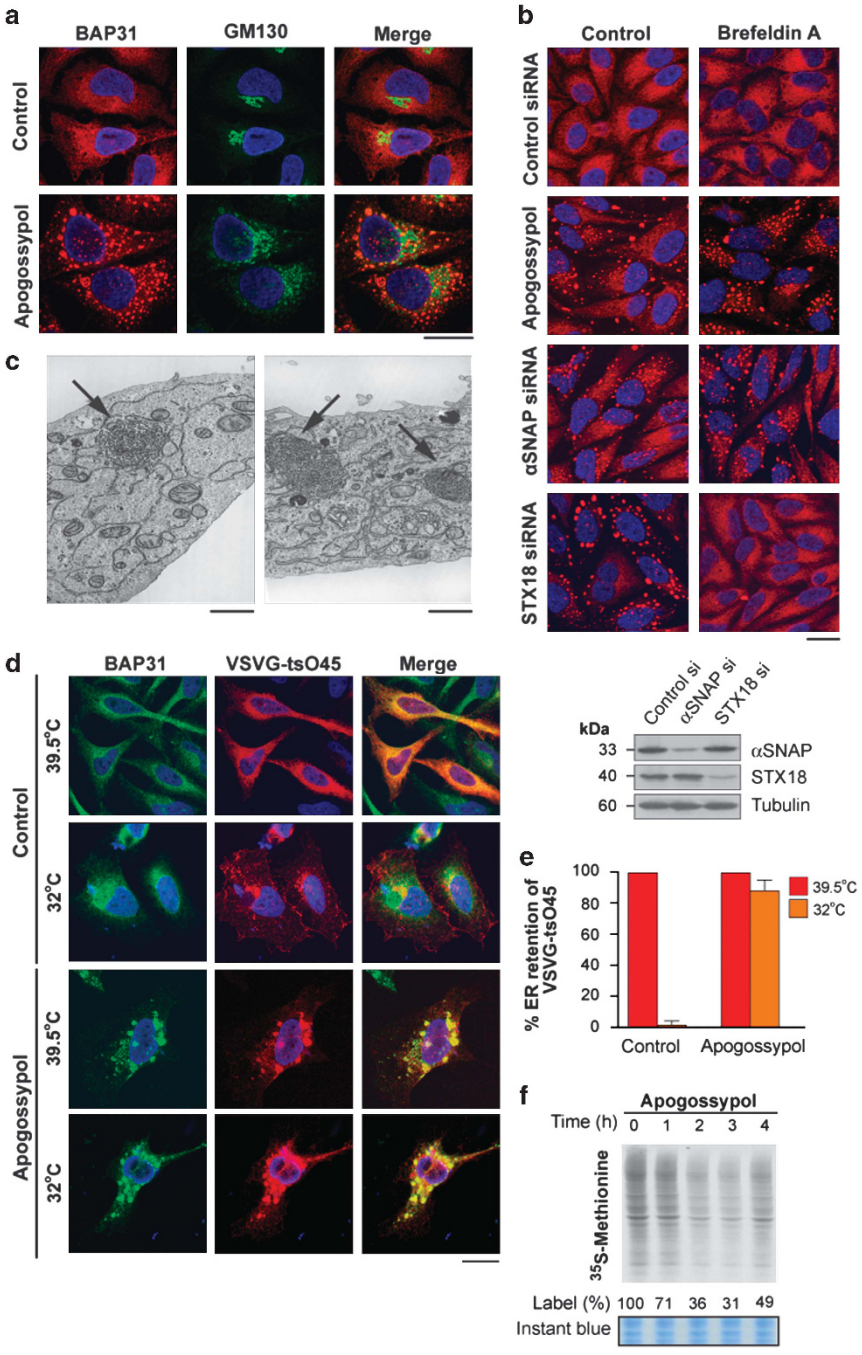

Figure 2 Apogossypol disrupts ER transport and function. (**a**) HeLa cells, exposed for 4 h to apogossypol (10 μM), were immunostained for membrane proteins in the ER (BAP31) and Golgi (GM130). Cells with BAP31 aggregates exhibited a near complete dispersal of Golgi (scale bar, 20 μm). (**b**) Disruption of trafficking, by downregulation of αSNAP and STX18, resulted in the formation of BAP31 membrane aggregates similar to those following exposure to apogossypol (scale bar, 20 μm). Exposure to brefeldin A (20 μM) for 0.5 h completely dispersed BAP31-containing aggregates in the STX18 but not in αSNAP downregulated or apogossypol-treated cells, consistent with defects in anterograde rather than retrograde trafficking (scale bar, 20 μm). The loss of the respective proteins was confirmed by western blotting (lower panel). (**c**) Downregulation of αSNAP (left panel) and STX18 (right panel) by RNAi resulted in the formation of ER membrane aggregates (black arrows) (scale bar, 1 μm) (**d**) ER membrane aggregates disrupt ER to Golgi trafficking. HeLa cells transfected with VSVG-ts045-Cherry construct and maintained at the restrictive (39.5 °C) temperature were exposed to apogossypol (10 μM) for 2 h and shifted to permissive (32 °C) temperature for another 2 h. The cells were then fixed and immunostained for BAP31, and assessed by confocal microscopy (scale bar, 20 μm). (**e**) The graph shows the ER retention of VSVG protein following a shift from the restrictive (39.5 °C) to permissive (32 °C) temperature in control and treated cells, from an average of a minimum of 200 cells from three independent experiments; error bars show the S.D. (**f**) Apogossypol induced a global attenuation of translation, as depicted in the autoradiogram. Autoradiography of [^{35}S] methionine-labelled proteins in lysates of HeLa cells exposed to apogossypol (10 μM) for 1–4 h were resolved by NuPage. Data were expressed as a percentage of [^{35}S]-labelling of HeLa cells not exposed to ApoG following Phosphorimager analysis. Lower panel is a photomicrograph of an instant blue-stained gel, showing equal loading

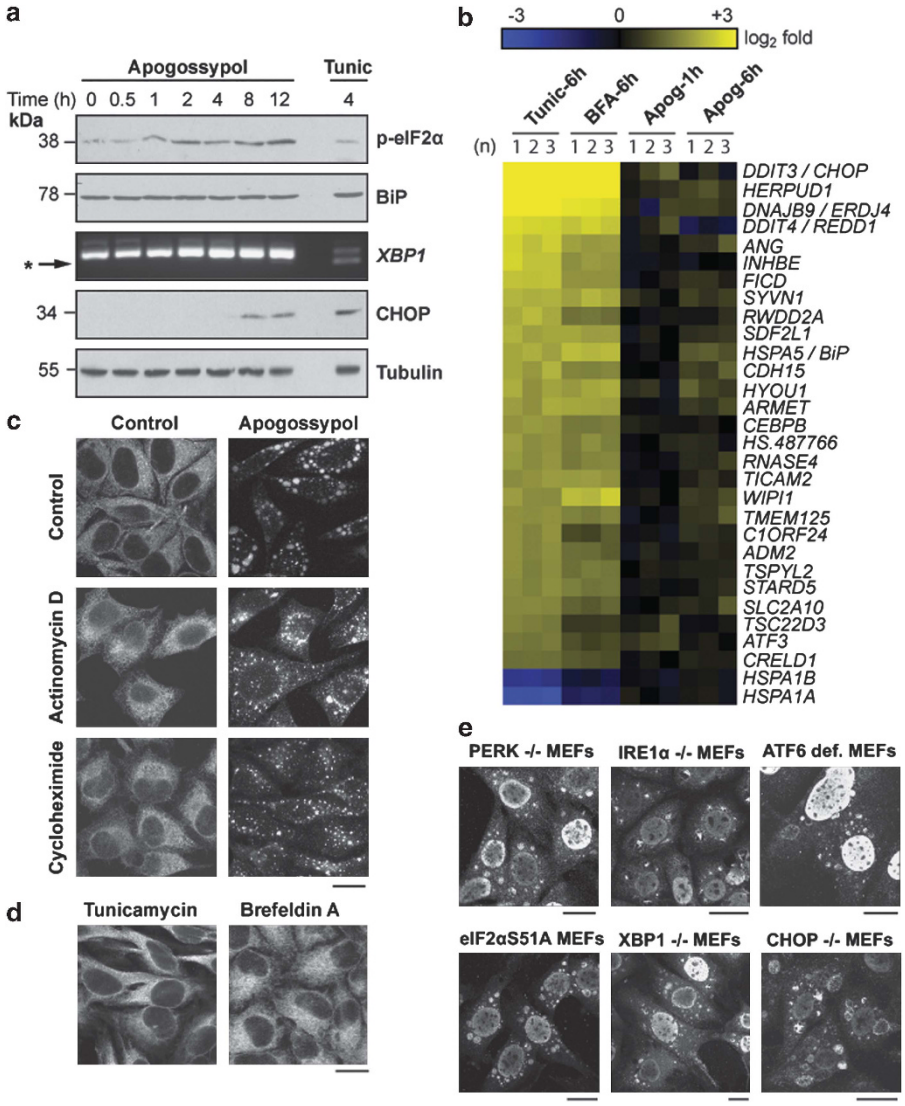

Figure 3 Apogossypol induces a novel form of ER stress distinct from the classical UPR. (**a**) Most biochemical changes associated with canonical ER stress occur much later than the induction of ER membrane aggregates at 1 h. Whole-cell lysates or total RNA of HeLa cells exposed to apogossypol (10 μM) or tunicamycin (20 μM) for the indicated times were either immunoblotted with the indicated antibodies, or analysed by RT-PCR using a primer set that amplified human *XBP1* mRNA. Unspliced and IRE1-spliced *XBP1* (*) transcripts yield 289 and 263-bp products, respectively. (**b**) Apogossypol (1 h) induced very few gene changes associated with canonical ER stress despite extensive ER membrane aggregation. Heat map analysis comparing gene changes following 6 h of tunicamycin (20 μM) or brefeldin A (20 μM) to 1 or 6 h of apogossypol (10 μM) treatment in MCF-7 cells, where yellow and blue indicate up- or downregulation, respectively. Tunicamycin and brefeldin A markedly altered many characteristic ER stress genes, whereas apogossypol changed a few of these genes and to a much lesser degree. Analysis from three separate experiments (*n*) was used to generate the heat map. (**c**) Apogossypol induces ER membrane aggregation in the absence of transcription or translation, as evidenced by a 4-h pre-treatment of actinomycin D (10 μM) or cycloheximide (20 μM) followed by another 4 h to apogossypol (10 μM) (scale bar, 20 μm). (**d**) Two classical inducers of canonical ER stress, tunicamycin (20 μM) and brefeldin A (20 μM), failed to induce ER membrane aggregation (scale bar, 20 μm). (**e**) Knockout of genes critical for canonical ER stress did not affect the ability of apogossypol to induce ER membrane aggregation. After 4 h, apogossypol (20 μM) induced ER membrane aggregation in PERK $-/-$, eIF2α S51A, IRE1α $-/-$, XBP1 $-/-$, CHOP $-/-$ and ATF6-deficient murine embryonic fibroblasts (scale bar, 10 μm)

absence of transcription or translation, in marked contrast to the UPR (Figure 3c), and conventional UPR inducers failed to induce ER membrane reorganisation (Figure 3d), thus confirming that the UPR is not a prerequisite for ER membrane reorganisation. Rather, ER membrane reorganisation occurs even when the UPR is inactivated by inhibiting transcription and translation. Finally, apogossypol induced ER membrane reorganisation in cells lacking PERK, phosphorylatable eIF2α, IRE1, XBP1, ATF6 or CHOP (Figure 3e), thus negating all the arms of the UPR, including eIF2α phosphorylation, in the formation of membrane aggregates. Taken together, these data demonstrate that ER membrane aggregation is a novel paradigm of cellular stress, which is associated with a major reorganisation of the ER and independent of the classical ER stress pathway.

MCL-1 regulates ER membrane reorganisation. Like apogossypol, another pan BCL-2 family antagonist,

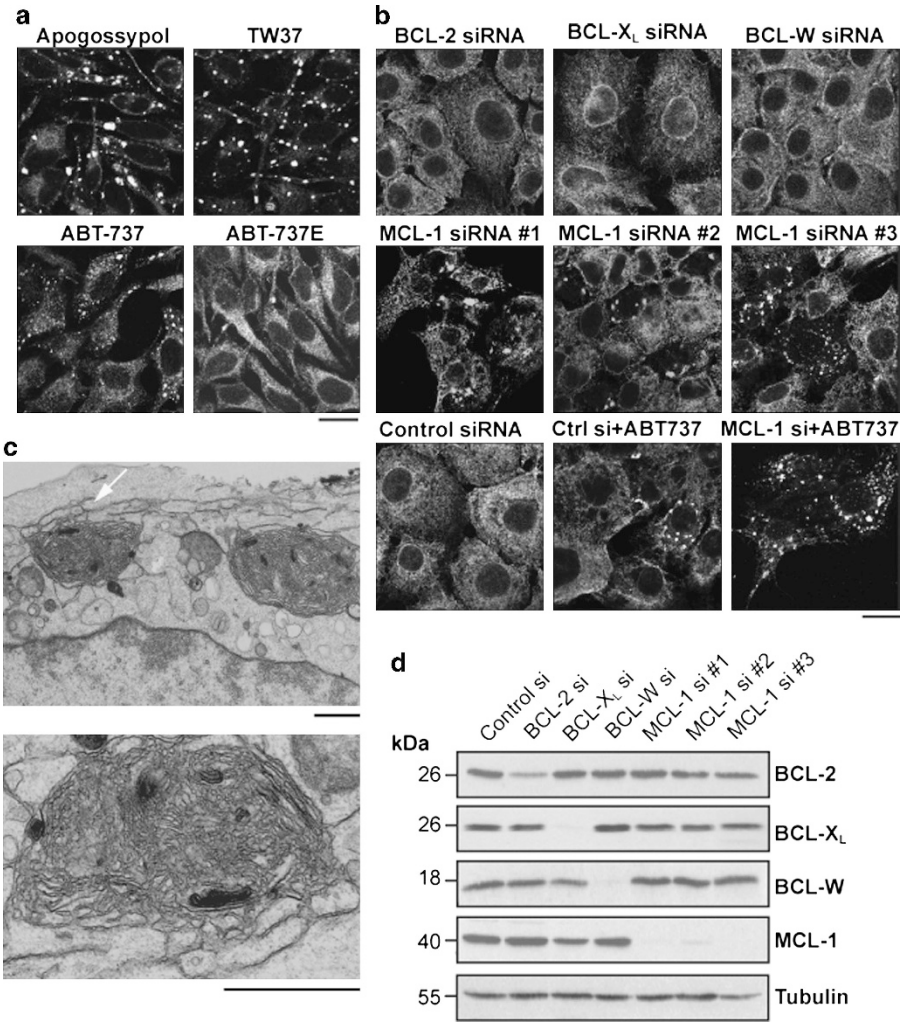

Figure 4 MCL-1 is a key anti-apoptotic BCL-2 family member that regulates ER membrane reorganisation. (**a**) Pan-BCL-2 family inhibitors induce ER membrane reorganisation more potently than BCL-2 and BCL-X$_L$-specific inhibitors. Apogossypol (10 μM) and TW37 (20 μM) induced extensive membrane reorganisation, assessed by BAP31 staining in HeLa cells, within 4 h of exposure, whereas ABT-737 (20 μM) induced modest reorganisation after 8 h and the inactive enantiomer ABT-737E (20 μM) failed to induce reorganisation (scale bar, 20 μm). (**b**) MCL-1 is the most important anti-apoptotic BCL-2 family member involved in the regulation of ER membrane reorganisation. HeLa cells following 72 h silencing of BCL-2, BCL-XL or BCL-W did not exhibit detectable ER modification, whereas ER membrane reorganisation was induced by three independent siRNAs of MCL-1 and this was potentiated by ABT-737 (scale bar, 20 μm). (**c**) The nature of the ER membrane reorganisation resulting from MCL-1 knockdown in MCF7 cells was confirmed by electron microscopy. A detail of a membrane aggregate in the upper panel is shown in the lower panel (scale bars, 1 μm). (**d**) Western blots confirmed the efficiency of the siRNA oligoduplexes

TW37,[21] also resulted in extensive ER membrane reorganisation within 4 h (Figure 4a). Interestingly, ABT-737, which inhibits BCL-2, BCL-X$_L$ and BCL-W but not MCL-1or BCL2-A1,[21,22] induced a lower incidence of ER reorganisation after longer exposure times (8 h) and the inactive enantiomer of ABT-737 failed to induce these aggregates (Figure 4a), suggesting the involvement of multiple BCL-2 family members in the formation of the ER membrane aggregates, in a BH3-dependent manner. Although the binding affinities of these antagonists vary widely,[12,13] there was no clear correlation between inhibition of a particular BCL-2 family member and ER membrane reorganisation. To establish the roles of specific members of the BCL-2 family, we used RNA interference to downregulate anti-apoptotic BCL-2 family members. Silencing of MCL-1, but not BCL-2, BCL-X$_L$ or BCL-W, resulted in ER membrane reorganisation, which was confirmed using three independent siRNA oligoduplexes for MCL-1 (Figures 4b–d). Downregulation of MCL-1 resulted in the formation of ER membrane reorganisation in $\sim$30% of the cells, which was enhanced to $\sim$70% following simultaneous inhibition of other BCL-2 family members with ABT-737 (Figure 4b). Taken together, these data support a role for other BCL-2 family members in addition to MCL-1 in the regulation of ER membrane reorganisation.

Connectivity mapping identifies chemicals that induce ER membrane reorganisation. To identify other regulators of this novel stress response, we used connectivity mapping to compare the mRNA signature from cells exposed to apogossypol with a database containing signatures from $>$1400 chemicals.[23] When the top 30 differentially expressed genes following apogossypol (Supplementary Table S1) were used

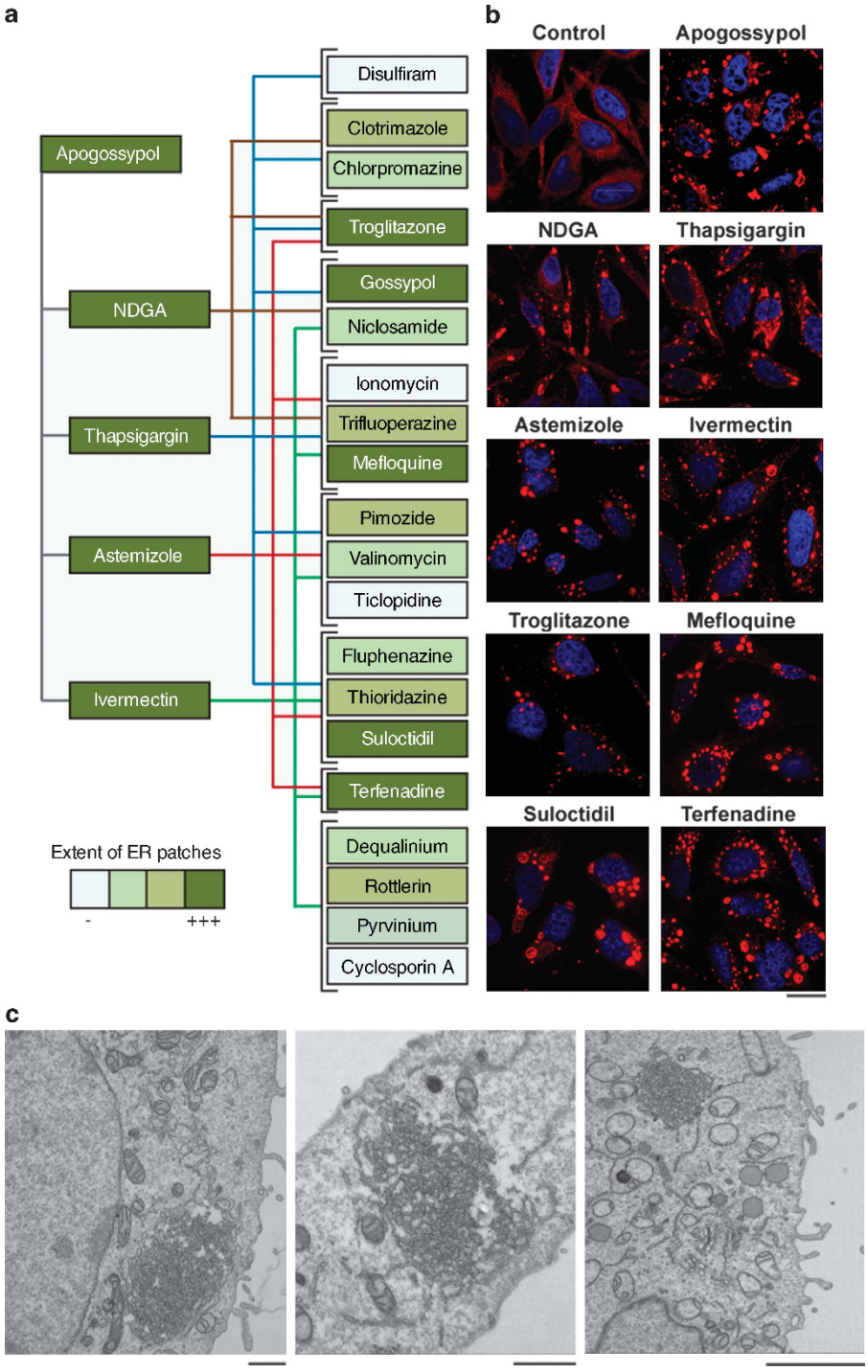

Figure 5 Chemical connectivity mapping identifies compounds from diverse chemical classes that induce ER membrane reorganisation. (**a**) The connectivity map identified 24 chemicals of which 20 were positive when tested for their ability to induce ER membrane reorganisation. Scheme representing the connectivity map of apogossypol (grey lines), NDGA (brown lines), THG (blue lines), astemizole (red lines) and ivermectin (green lines) with several compounds contained within the connectivity reference database. All boxes are colour coded in increasing shades of green to demonstrate the extent of ER membrane reorganisation, in HeLa cells after 4 h exposure to the indicated chemical, from no (−) to extensive aggregation (+++). (**b**) Exposure of HeLa cells for 4 h to apogossypol (10 μM), NDGA (50 μM), THG (10 μM), astemizole (5 μM), ivermectin (20 μM), troglitazone (20 μM in serum-free media), mefloquine (20 μM), suloctidil (20 μM) and terfenadine (10 μM) exhibited varying levels of ER membrane reorganisation assessed by BAP31 staining (scale bar, 20 μm). (**c**) Ultrastructural analysis confirmed that these BAP31 clusters induced by NDGA (left panel, scale bar, 1 μm), THG (middle panel, scale bar, 1 μm) and rottlerin (right panel, scale bar, 2 μm) were *bona fide* ER membrane aggregates

to interrogate the database,[24,25] we identified strong positive connections with structurally unrelated compounds, including nordihydroguaiaretic acid (NDGA), thapsigargin (THG), astemizole and ivermectin (Figure 5a), all of which induced extensive ER membrane reorganisation (Figure 5b). Therefore their genomic signatures were compiled (Supplementary

Table S1) using gene transcription data from the existing connectivity map reference database[23] and queried to select a further 20 compounds (Figure 5a). Remarkably 20/24 compounds identified by the connectivity map induced ER membrane reorganisation (Figures 5a–c and data not shown), demonstrating the wide-spread occurrence of this stress response. As the compounds identified by connectivity mapping are structurally and functionally diverse, it is likely that these chemicals regulate membrane reorganisation by different mechanisms, including perturbation of calcium homeostasis, a property shared by many of these chemicals. Both cyclopiazonic acid and 2,5-di-*t*-butyl-1,4-benzohydroquinone, inhibitors of SERCA ATPase activity, like THG, induced ER membrane reorganisation (Supplementary Figure S2a), suggesting that depletion of ER calcium stores could also regulate ER membrane reorganisation. However, this is not a prerequisite for ER membrane reorganisation, as apogossypol, unlike THG, neither increased cytosolic-free calcium nor depleted ER calcium stores (Supplementary Figures S2b and S2c).

ER membrane reorganisation perturbs hERG trafficking and function. Interestingly, a careful examination of the compounds identified by connectivity mapping revealed that a significant number of these are associated with cardiotoxicity (Figure 6a). Specifically, many of these compounds induce a cardiac abnormality called LQTS,[26,27] which is diagnosed on the basis of lengthening of the QT interval on electrocardiograms. LQTS results from delayed cardiac ventricular action potential repolarisation, owing to abnormalities of ion channel function, and is associated with ventricular arrhythmias and sudden death.[26,27] Drugs that induce LQTS primarily block the hERG (human ether-a-go-go-related gene) channel pore thereby inhibiting the rapid delayed rectifier K current (I_{Kr}), which is crucial for terminating the action potential.[28] However, recent evidence also implicates defective hERG trafficking in the induction of LQTS.[29–31] As apogossypol-induced ER membrane reorganisation resulted in impaired ER transport (Figure 2e), we speculated that ER membrane reorganisation could interfere with the trafficking and normal functioning of hERG channels at the cell surface. Indeed, in HEK293 cells stably transfected with hERG, apogossypol caused a major redistribution of the ER-resident hERG protein to BAP31-positive clusters, suggesting a trafficking defect of membrane-bound hERG channels (Figure 6b). Similarly, the antihistamine terfenadine, but not its metabolite, fexofenadine, induced ER membrane reorganisation with hERG associated with the ER membrane aggregates (Figure 6b). Interestingly, terfenadine has been withdrawn from the market owing to its cardiotoxic side effects and replaced by fexofenadine, which has a much lower binding affinity for hERG. These results raised the distinct possibility that agents that induce ER membrane reorganisation may induce LQTS. To investigate this, we sought to determine if apogossypol reduced hERG channel function at the cell surface. Apogossypol dramatically reduced hERG currents (Figure 6c) and also reduced the cell size determined by membrane capacitance measurements. Furthermore, hERG current amplitudes normalised for differences in capacitance (current density) were significantly ($P<0.0001$) reduced from 63.2 ± 7.4 pA/pF ($n=18$) to 11.2 ± 2.8 pA/pF ($n=16$) (Figures 6c and d), providing direct evidence of a dramatic disruption of channel trafficking and a novel mechanism of drug-induced LQTS.

Discussion

Although numerous reports have demonstrated the ability of cells to induce the UPR, following excessive accumulation of unfolded proteins,[5,6] ultrastructural changes associated with canonical ER stress and the UPR have largely been limited to ER lumen swelling. We now report a novel, evolutionarily conserved, cellular stress response characterised by rapid and reversible reorganisation of ER membranes into massive aggregates of convoluted ER tubules (Figure 1 and Supplementary Figure S1). Although ER membrane reorganisation is induced by pan-BCL-2 antagonists and many other chemicals identified by connectivity mapping (Figures 4 and 5), it is important to note that this cellular stress response is not solely a consequence of chemical exposure. Rather, it is part of a dynamic homeostatic response occurring in physiological conditions, including altered vesicular trafficking[19] (Figure 2). ER membrane reorganisation is distinct from the membrane whorls observed in organised smooth ER and phospholipidosis[32] and shows no indications of apoptosis or autophagy (data not shown). Most importantly, ER membrane reorganisation clearly differs from canonical ER stress and the UPR as it occurs without the biochemical characteristics of the UPR, in the absence of transcription or translation and in cells lacking genes critical for induction of the UPR (Figure 3). Nonetheless, some features of canonical ER stress become evident at later times following ER membrane reorganisation, suggesting that ER membrane reorganisation occurs upstream and/or independent of the UPR. In addition, the aggregated ER membranes result in functional perturbation of the ER with potential pathological consequences (Figures 2 and 6), characteristic of a novel cellular stress response.

Our results highlight a novel role for BCL-2 family members, particularly MCL-1, in regulating ER membrane reorganisation, representing an unrecognised physiological function[33] of some BCL-2 family members (Figure 4). However, a handful of disparate reports describing similar ER structural changes (Supplementary Table S2), along with our observation of ER membrane reorganisation in yeast, which lacks BCL-2 family proteins, suggest that this stress response is not restricted to BCL-2 family inhibition. Using connectivity mapping, we demonstrate that ER membrane reorganisation is a common cellular response occurring following exposure to diverse pharmacological agents, including antipsychotics (chlorpromazine, trifluoperazine, pimozide, fluphenazine and thioridazine), antihistamines (astemizole and terfenadine), antimalarials (mefloquine) and antiparasitics (ivermectin) (Figure 5). Moreover, as we only tested 24 chemicals from the connectivity map, identification of 20 ER membrane aggregating agents is certainly a gross underestimate of the number of chemicals able to induce this novel stress pathway. These compounds probably regulate ER membrane reorganisation by several mechanisms, including BCl-2 family inhibition, trafficking defects[34] and altered lipid metabolism,[35]

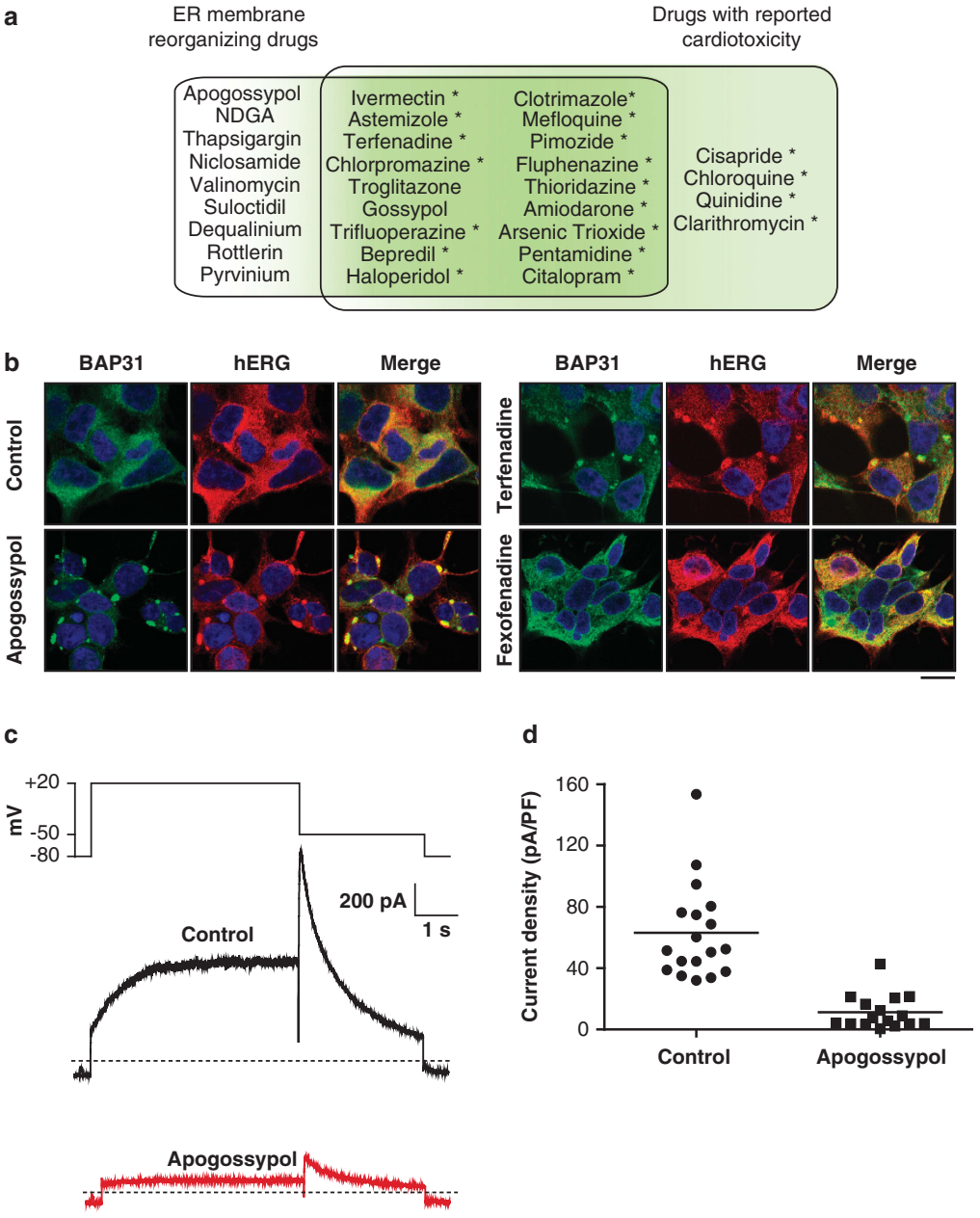

Figure 6 ER membrane reorganisation leads to hERG trafficking and functional defects. (**a**) Most agents that induce ER membrane reorganisation are associated with cardiotoxicity as illustrated by the degree of overlap in the scheme. The drugs implicated in causing LQTS are marked with an asterisk (*). Some of the ER membrane reorganisation agents in the left-hand panel have not been tested for their ability to induce LQTS. (**b**) hERG colocalised with ER membrane aggregates in apogossypol- and terfenadine- but not fexofenadine-treated cells. HEK293 cells, stably expressing hERG, were exposed for 4 h to either apogossypol (10 μM), terfenadine (10 μM) or fexofenadine (10 μM), and immunostained for BAP31 and hERG (scale bar, 20 μm). (**c**) Voltage clamp measurements reveal that hERG currents are greatly reduced in apogossypol-treated cells compared with untreated cells. Currents were elicited with 5-s voltage steps to $+20$ mV and peak tail currents measured upon repolarisation to -50 mV. (**d**) The decreases in hERG channel function are owing both to a decrease in cell size (as indicated by reductions in membrane surface area and capacitance) and also owing to reduced channel numbers. Tail current densities (peak tail current amplitude divided by capacitance) for individual cells are substantially attenuated in apogossypol-treated cells. Each data point in the scatter plots represents a measurement from a single cell. The mean current densities for each group are illustrated by the horizontal lines

thus characterising ER membrane reorganisation as a widespread cellular stress response with complex regulatory mechanisms (Figure 7).

It is hardly surprising that such a dramatic and widespread cellular response could lead to important pathological consequences. The high degree of overlap between drugs inducing ER membrane reorganisation and those with associated cardiotoxicity, particularly LQTS (Figure 6a), suggested the possibility that ER membrane reorganisation may be a novel mechanism responsible for their cardiotoxic

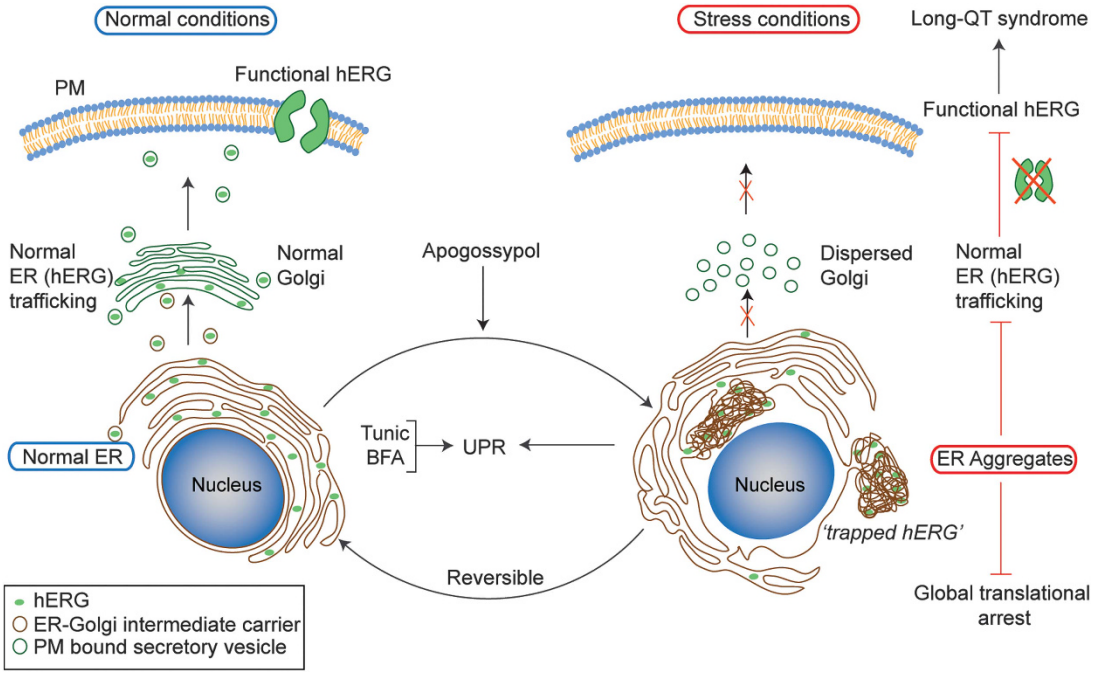

Figure 7 Scheme representing the formation, regulation and consequences of ER membrane reorganisation. Under normal conditions, proteins, such as hERG, are synthesised in the ER lumen, and trafficked via the Golgi to the plasma membrane (PM) to express a functional channel (left-hand panel). Exposure to stress conditions, such as inhibition of the BCL-2 family (apogossypol and TW37), induced ER membrane reorganisation (right-hand panel). This ER membrane reorganisation is reversible and occurs independent of canonical ER stress, as tunicamycin (Tunic) and brefeldin A (BFA), two inducers of canonical ER stress, do not result in ER membrane reorganisation. However, at later times, the extensive ER membrane reorganisation may eventually lead to canonical ER stress and the UPR, thus placing ER membrane reorganisation upstream and/or independent of the UPR. Furthermore, ER membrane reorganisation results in the functional perturbation of the ER, characterised by a near complete dispersion of the Golgi and an accompanying trafficking defect. This novel cellular stress pathway could lead to important pathological consequences, including LQTS, mediated by the entrapment of the newly synthesised hERG in the aggregates resulting in a trafficking defect that is marked by the loss of functional hERG channels at the cell surface

side effects. Drug-induced LQTS involves a loss of function of specific cell surface ion channels, particularly hERG, resulting in ventricular arrhythmias and death.[26,27] This loss of function is normally brought about by either the direct binding of the drugs to the hERG channel pore, or by a trafficking defect of the newly synthesised hERG from the ER to the cell surface. On acute application, apogossypol exhibited only very weak inhibition to hERG currents by direct channel block (data not shown), compared with the marked inhibition following trafficking defects induced by ER reorganisation (Figures 6b–d). Thus, our results implicate ER membrane reorganisation and the subsequent arrest in hERG trafficking as a novel mechanism to induce LQTS, although further studies are required to confirm this mechanism *in vivo*. Support for this is provided both by the finding that ivermectin and pentamidine, which induce LQTS by trafficking defects rather than channel block,[31] induce ER membrane reorganisation (Figure 6a and data not shown), and also terfenadine, but not its hERG-inactive metabolite, fexofenadine, resulted in hERG trafficking and functional defects (Figure 6b).

In this study, we have identified and characterised a new cellular stress response involving extensive ER membrane reorganisation. Remarkably, despite thousands of papers on canonical ER stress and the UPR, this new stress pathway also involving the ER has largely gone unrecognised, possibly because of its rapid formation and reversibility. The interaction and cross talk between these two forms of cellular stress that affect the ER may be an important area for future study. We have highlighted the effects of ER membrane reorganisation on protein trafficking from the ER with potential links to LQTS. However, this novel cellular stress pathway with its redistribution and clustering of specific ER membrane proteins may also disrupt other ER functions, including receptor recycling, protein secretion, lipid metabolism, drug detoxification and the association of ER with other cellular organelles, with potentially important functional and pathological consequences. Moreover, redistribution and clustering of specific ER membrane proteins may interfere with their normal functions. For example, clustering of BAP31 could interfere with its ability to promote the retrotranslocation of ER-resident proteins to the cytosol for subsequent proteasomal degradation.[36] Similarly, aggregation of RTN4 may well be involved in the structural changes observed in the present study by interfering with the shaping of tubular ER[2] or with vesicular trafficking.[37] Taken together, it is apparent that further understanding of this novel cellular stress response may well hold the key for several important questions pertaining to ER structure, function, vesicular trafficking and pathology.

Materials and Methods

Cell culture. HeLa and MCF7 cells from ATCC (Middlesex, UK), PERK-, IRE1α- and CHOP-null MEFs from Drs D Ron and H Harding (University of Cambridge, UK), eIF2α S51A MEFs from Dr R Kaufman (Burnham Institute, La Jolla, CA, USA), ATF6-deficient and XBP1-null MEFs from Dr L Glimcher (Harvard Medical School, MA, USA), and HEK293, stably transfected with hERG

from Professor. C January (University of Wisconsin, WI, USA), were cultured in DMEM medium supplemented with 5 mM L-glutamine and 10% fetal calf serum (all from Life Technologies Inc., Paisley, UK). Chinese hamster ovary cells, from Dr J Downward (Cancer Research UK, London Research Institute, London, UK), were cultured in RPMI 1640 medium supplemented with 10 % fetal calf serum and 5 mM L-glutamine. Lymphocytes purified from blood samples of patients with CLL were cultured as previously described.[15] Wild-type *S. pombe* cells (KT301: *h*^{90} *ade6.M216 leu1.32*) were cultured in medium[38] supplemented with adenine and leucine, until the cell density reached 2×10^6 cells/ml, before drug exposure.

Reagents and plasmids. Apogossypol was synthesised as described.[39] TW37 was from Selleck Chemicals LLC (Houston, TX, USA). ABT-737 and its inactive enantiomer were kind gifts (Dr S Rosenberg, Abbott Laboratories, Abbott Park, IL, USA). CFP- SEC20 and 22 constructs were from Dr G Mollard (Universität Bielefeld, Bielefeld, Germany). ER-Red plasmid was from Clontech (Mountain View, CA, USA). VSVG-ts045-Cherry was from Dr S Bratton (University of Texas at Austin, TX, USA). Antibodies against human BAP31, αSNAP and CHOP from Abcam (Cambridge, UK); mouse BAP31 from Dr G Shore (McGill University, Quebec, Canada); Calnexin, HSP60, EEA1, GM130 and BCL-x_L from BD Biosciences (Oxford, UK); RTN4, hERG and MCL-1 from Santacruz (Santacruz, CA, USA); BCL-w, Tubulin and RAB7 from Cell Signaling (Danvers, MA, USA); ERGIC53 from Sigma (St. Louis, MO, USA); BCL-2 from Dako (Ely, UK); STX18 from Synaptic Systems (Goettingen, Germany) and CD63 from Developmental Studies Hybridoma Bank (Iowa city, IA, USA) were used. All other reagents, unless mentioned otherwise, were from Sigma-Aldrich Co. (St. Louis, MO, USA).

Transient overexpression and siRNA knockdowns. For transient transfections, cells were transfected using TransIT-LT-1 transfection reagent (Mirus Bio LLC, Madison, WI, USA) and left for 48 h, according to the manufacturer's instructions. For siRNA knockdowns, cells were reverse-transfected with oligoduplexes (Life Technologies Inc.), using Interferin Reagent (Polyplus transfection Inc., New York, NY, USA), according to the manufacturer's protocol and processed 72 h after transfection. Cells were reverse-transfected with 10 nM of αSNAP (ID# S16714), STX18 (ID# S28735), BCL-2 (ID# S224526), BCL-w (ID# S1924), BCL-X_L (pool of three siRNAs) or three siRNAs of MCL-1 (ID# S8583, S8585 and a pool of three siRNAs).

RT-PCR and XBP1 splicing. Total RNA extracted (RNAeasy, Qiagen, Hilden, Germany) from cells exposed to apogossypol or tunicamycin was reverse-transcribed (Invitrogen, Carlsbad, CA, USA), and the resulting cDNA used as a template for PCR amplification using primers 5′-TTACGAGAGAAAACTCA TGGC-3′ and 5′-GGGTCCAAGTTGTCCAGAATGC-3′ to generate the 289-bp amplicon of spliced *XBP1,* which was resolved on a 2.5% agarose/1 × TAE gel and visualised.

Western blotting. Western blots were carried out according to standard protocols.[15] Briefly, 50 μg of total protein lysate was subjected to SDS-PAGE electrophoresis. Subsequently, proteins were transferred to nitrocellulose membrane and protein bands visualised with ECL reagents (GE Healthcare, Bucks, UK).

Microscopy. For immunofluorescent staining, cells grown on coverslips were fixed with 4% (v/v) paraformaldehyde, permeabilised with 0.5% (v/v) Triton X-100 in PBS and followed by incubations with primary antibodies, the appropriate fluorophore-conjugated secondary antibodies, mounted on glass slides and subjected to confocal microscopy on a Zeiss LSM510 (Cambridge, UK). For electron microscopy, cells were fixed and processed as described previously.[15] Electron micrographs were recorded using an ES1000W CCD camera and DigitalMicrograph software (Gatan, Abingdon, UK) in a Zeiss 902A electron microscope.

VSVG trafficking assay. Cells transfected with VSVG-ts045-Cherry constructs were kept at 39.5 °C for 16 h, treated with DMSO or apogossypol and maintained at 39.5 °C or shifted to 32 °C for the indicated times. Retention of VSVG protein in the ER was recorded. In each case, at least 200 cells were monitored and graphs plotted from averages of three independent experiments.

Assessment of translation rates. HeLa cells were plated as for immunoblot analyses, treated as indicated, labelled with 30.6 μCi/ml [^{35}]S-methionine (EasyTag, PerkinElmer, Waltham, MA, USA) for 10 min at 37 °C, washed with ice-cold PBS and lysed in 75 μl Laemmli Buffer. Lysates were sonicated, boiled at 95 °C for 5 min and resolved on 4–12% NuPAGE gradient gels (Invitrogen). Gels were then stained with Instant blue and analysed by phosphorimaging.

Microarray analysis, connectivity mapping and statistics. Total RNA extracted from MCF7 cells exposed to different agents was used to make biotin-labelled cRNA using the Illumina TotalPrep RNA amplification kit, hybridised to an Illumina HumanHT-12 BeadChip array, Cy3 labelled and scanned using an Illumina BeadArray Reader (all from Illumina, Hayward, CA, USA). Microarray data normalisation and analyses were carried out using ArrayTrack software (NCTR/FDA, Jefferson, AR, USA), and the data sets were compared by Welch *t*-test. For heat map analysis, the top 30 genes with the highest fold changes ($P < 0.003$) following tunicamycin treatment were compiled and compared with the transcriptional changes in cells exposed to brefeldin A and apogossypol using MultiExperiment Viewer (Boston, MA, USA). For connectivity mapping, the top 30 genes with the highest fold changes, deemed significant ($P < 0.05$) following apogossypol, were used to query a multi-platform-optimised version of build 2 of the Broad institute reference data set,[23] using the sscMap connectivity algorithm.[24,25] The top 30 genes with the highest fold changes for each of the high positive connections (NDGA, THG, astemizole and ivermectin) were collected from the database and queried to identify other compounds.

Patch clamping. Surface expression of functional hERG channels was determined by measuring hERG current amplitudes using the whole-cell configuration of the patch-clamp technique as described previously,[40] in stably transfected HEK 293 cells. Cells exposed to DMSO (control) or apogossypol for 16 h were lifted off the plate using enzyme-free cell dissociation buffer (Invitrogen) and transferred to the recording chamber. Cells were superfused with room temperature extracellular Tyrode containing (in mM), NaCl 140, $MgCl_2$ 1, KCl 4, glucose 10, HEPES 5, $CaCl_2$ 2, pH 7.4. Borosilicate glass pipettes were filled with an intracellular solution containing (in mM), KCl 130, MgATP 5, HEPES 10, pH 7.2. Peak tail current amplitudes were measured and leak current subtracted. Membrane capacitance was measured as an index of cell membrane surface area using the series resistance and capacitance compensation circuitry of the patch clamp amplifier (Axopatch 200B, Molecular Devices, Sunnyvale, CA, USA) and used to determine current density (current normalised to capacitance). Recordings were made for up to a maximum of 4 h following removal of cells from culture.

Calcium imaging. HeLa cells grown on coverslips were loaded with 2 μM Fura-2 AM (Life Technologies Inc.) in extracellular medium, containing (in mM) NaCl 121, KCl 5.4, $MgCl_2$ 1.6, $CaCl_2$ 1.8, $NaHCO_3$ 6, glucose 9, HEPES 25, pH 7.4, in the dark at room temperature for 30 min, washed, mounted on a Zeiss axiovert inverted microscope and maintained at 37 °C in extracellular medium. Epifluorescent images were collected with alternating excitation at 340 and 380 nm and emissions above 510 nm using a digital CCD camera (Orca ER, Hamamatsu, Hamamatsu city, Japan). Data were converted to 340/380 pseudocolour ratiometric images using MetaFluor software (Molecular Devices, Sunnyvale, CA, USA). For all experiments, changes in cytosolic calcium were measured in 20 individual cells in at least three separate experiments.

Conflict of Interest

The authors declare no conflict of interest.

Acknowledgements. We thank Drs Bratton, Downward, Glimcher, Harding, Mollard, Rosenberg and Shore for cells and reagents, and Professor A Willis for helpful discussions. We thank Judy McWilliam, Tim Smith and Kate Phillips for technical assistance, and the Medical Research Council for core support. We thank the NIH (grant CA149668 to MP) for support.

1. Hu J, Prinz WA, Rapoport TA. Weaving the web of ER tubules. *Cell* 2011; **147**: 1226–1231.
2. Voeltz GK, Prinz WA, Shibata Y, Rist JM, Rapoport TA. A class of membrane proteins shaping the tubular endoplasmic reticulum. *Cell* 2006; **124**: 573–586.
3. Baumann O, Walz B. Endoplasmic reticulum of animal cells and its organization into structural and functional domains. *Int Rev Cytol* 2001; **205**: 149–214.

4. Lynes EM, Simmen T. Urban planning of the endoplasmic reticulum (ER): how diverse mechanisms segregate the many functions of the ER. *Biochim Biophys Acta* 2011; **1813**: 1893–1905.
5. Ron D, Walter P. Signal integration in the endoplasmic reticulum unfolded protein response. *Nat Rev Mol Cell Biol* 2007; **8**: 519–529.
6. Schroder M, Kaufman RJ. The mammalian unfolded protein response. *Annu Rev Biochem* 2005; **74**: 739–789.
7. McCullough KD, Martindale JL, Klotz LO, Aw TY, Holbrook NJ. Gadd153 sensitizes cells to endoplasmic reticulum stress by down-regulating Bcl2 and perturbing the cellular redox state. *Mol Cell Biol* 2001; **21**: 1249–1259.
8. Puthalakath H, O'Reilly LA, Gunn P, Lee L, Kelly PN, Huntington ND *et al.* ER stress triggers apoptosis by activating BH3-only protein Bim. *Cell* 2007; **129**: 1337–1349.
9. Oakes SA, Lin SS, Bassik MC. The control of endoplasmic reticulum-initiated apoptosis by the BCL-2 family of proteins. *Curr Mol Med* 2006; **6**: 99–109.
10. Rong Y, Distelhorst CW. Bcl-2 protein family members: versatile regulators of calcium signaling in cell survival and apoptosis. *Annu Rev Physiol* 2008; **70**: 73–91.
11. Youle RJ, Strasser A. The BCL-2 protein family: opposing activities that mediate cell death. *Nat Rev Mol Cell Biol* 2008; **9**: 47–59.
12. Lessene G, Czabotar PE, Colman PM. BCL-2 family antagonists for cancer therapy. *Nat Rev Drug Discov* 2008; **7**: 989–1000.
13. Vogler M, Dinsdale D, Dyer MJ, Cohen GM. Bcl-2 inhibitors: small molecules with a big impact on cancer therapy. *Cell Death Differ* 2009; **16**: 360–367.
14. Albershardt TC, Salerni BL, Soderquist RS, Bates DJ, Pletnev AA, Kisselev AF *et al.* Multiple BH3 mimetics antagonize antiapoptotic MCL1 protein by inducing the endoplasmic reticulum stress response and up-regulating BH3-only protein NOXA. *J Biol Chem* 2011; **286**: 24882–24895.
15. Vogler M, Weber K, Dinsdale D, Schmitz I, Schulze-Osthoff K, Dyer MJ *et al.* Different forms of cell death induced by putative BCL2 inhibitors. *Cell Death Differ* 2009; **16**: 1030–1039.
16. Orrenius S, Ericsson JL, Ernster L. Phenobarbital-induced synthesis of the microsomal drug-metabolizing enzyme system and its relationship to the proliferation of endoplasmic membranes. A morphological and biochemical study. *J Cell Biol* 1965; **25**: 627–639.
17. Subramanian K, Meyer T. Calcium-induced restructuring of nuclear envelope and endoplasmic reticulum calcium stores. *Cell* 1997; **89**: 963–971.
18. Lippincott-Schwartz J, Liu W. Insights into COPI coat assembly and function in living cells. *Trends Cell Biol* 2006; **16**: e1–e4.
19. Iinuma T, Aoki T, Arasaki K, Hirose H, Yamamoto A, Samata R *et al.* Role of syntaxin 18 in the organization of endoplasmic reticulum subdomains. *J Cell Sci* 2009; **122**(Pt 10): 1680–1690.
20. Presley JF, Cole NB, Schroer TA, Hirschberg K, Zaal KJ, Lippincott-Schwartz J. ER-to-Golgi transport visualized in living cells. *Nature* 1997; **389**: 81–85.
21. Wang G, Nikolovska-Coleska Z, Yang CY, Wang R, Tang G, Guo J *et al.* Structure-based design of potent small-molecule inhibitors of anti-apoptotic Bcl-2 proteins. *J Med Chem* 2006; **49**: 6139–6142.
22. Oltersdorf T, Elmore SW, Shoemaker AR, Armstrong RC, Augeri DJ, Belli BA *et al.* An inhibitor of Bcl-2 family proteins induces regression of solid tumours. *Nature* 2005; **435**: 677–681.
23. Lamb J, Crawford ED, Peck D, Modell JW, Blat IC, Wrobel MJ *et al.* The Connectivity Map: using gene-expression signatures to connect small molecules, genes, and disease. *Science* 2006; **313**: 1929–1935.
24. Zhang SD, Gant TW. A simple and robust method for connecting small-molecule drugs using gene-expression signatures. *BMC Bioinformatics* 2008; **9**: 258.
25. Zhang SD, Gant TW. sscMap: an extensible Java application for connecting small-molecule drugs using gene-expression signatures. *BMC Bioinformatics* 2009; **10**: 236.
26. Kannankeril P, Roden DM, Darbar D. Drug-induced long QT syndrome. *Pharmacol Rev* 2010; **62**: 760–781.
27. Sanguinetti MC, Tristani-Firouzi M. hERG potassium channels and cardiac arrhythmia. *Nature* 2006; **440**: 463–469.
28. Mitcheson JS, Chen J, Lin M, Culberson C, Sanguinetti MC. A structural basis for drug-induced long QT syndrome. *Proc Natl Acad Sci USA* 2000; **97**: 12329–12333.
29. Dennis A, Wang L, Wan X, Ficker E. hERG channel trafficking: novel targets in drug-induced long QT syndrome. *Biochem Soc Trans* 2007; **35**(Pt 5): 1060–1063.
30. Rajamani S, Eckhardt LL, Valdivia CR, Klemens CA, Gillman BM, Anderson CL *et al.* Drug-induced long QT syndrome: hERG K + channel block and disruption of protein trafficking by fluoxetine and norfluoxetine. *Br J Pharmacol* 2006; **149**: 481–489.
31. Wible BA, Hawryluk P, Ficker E, Kuryshev YA, Kirsch G, Brown AM. HERG-Lite: a novel comprehensive high-throughput screen for drug-induced hERG risk. *J Pharmacol Toxicol Methods* 2005; **52**: 136–145.
32. Snapp EL, Hegde RS, Francolini M, Lombardo F, Colombo S, Pedrazzini E *et al.* Formation of stacked ER cisternae by low affinity protein interactions. *J Cell Biol* 2003; **163**: 257–269.
33. Hetz C, Glimcher L. The daily job of night killers: alternative roles of the BCL-2 family in organelle physiology. *Trends Cell Biol* 2008; **18**: 38–44.
34. Hatsuzawa K, Hirose H, Tani K, Yamamoto A, Scheller RH, Tagaya M. Syntaxin 18, a SNAP receptor that functions in the endoplasmic reticulum, intermediate compartment, and cis-Golgi vesicle trafficking. *J Biol Chem* 2000; **275**: 13713–13720.
35. Sprocati T, Ronchi P, Raimondi A, Francolini M, Borgese N. Dynamic and reversible restructuring of the ER induced by PDMP in cultured cells. *J Cell Sci* 2006; **119**(Pt 15): 3249–3260.
36. Wang B, Heath-Engel H, Zhang D, Nguyen N, Thomas DY, Hanrahan JW *et al.* BAP31 interacts with Sec61 translocons and promotes retrotranslocation of CFTRDeltaF508 via the derlin-1 complex. *Cell* 2008; **133**: 1080–1092.
37. Heidtman M, Chen CZ, Collins RN, Barlowe C. Yos1p is a novel subunit of the Yip1p-Yif1p complex and is required for transport between the endoplasmic reticulum and the Golgi complex. *Mol Biol Cell* 2005; **16**: 1673–1683.
38. Alfa C, Fantes P, Hyams J, McLeod M, Warbrick E. *Experiments with Fission Yeast: A Laboratory Course Manual.* Cold Spring Harbor Laboratory Press: Woodbury, NY, USA, 1993.
39. Becattini B, Kitada S, Leone M, Monosov E, Chandler S, Zhai D *et al.* Rational design and real time, in-cell detection of the proapoptotic activity of a novel compound targeting Bcl-X(L). *Chem Biol* 2004; **11**: 389–395.
40. Cockerill SL, Tobin AB, Torrecilla I, Willars GB, Standen NB, Mitcheson JS. Modulation of hERG potassium currents in HEK-293 cells by protein kinase C. Evidence for direct phosphorylation of pore forming subunits. *J Physiol* 2007; **581**(Part 2): 479–493.

Supplementary Information accompanies the paper on Cell Death and Differentiation website (http://www.nature.com/cdd)